

A combined analysis of the H_0 late time direct measurements and the impact on the Dark Energy sector

Eleonora Di Valentino¹*

¹*Institute for Particle Physics Phenomenology, Department of Physics, Durham University, Durham, DH1 3LE, UK.*

Accepted XXX. Received YYY; in original form ZZZ

ABSTRACT

We combine 23 Hubble constant measurements based on Cepheids-SN Ia, TRGB-SN Ia, Miras-SN Ia, Masers, Tully Fisher, Surface Brightness Fluctuations, SN II, Time-delay Lensing, Standard Sirens and γ -ray Attenuation, obtaining our best *optimistic* H_0 estimate, that is $H_0 = 72.94 \pm 0.75$ km/s/Mpc at 68% CL. This is in 5.9σ tension with the Λ CDM model, therefore we evaluate its impact on the extended Dark Energy cosmological models that can alleviate the tension. We find more than 4.9σ evidence for a phantom Dark Energy equation of state in the w CDM scenario, the cosmological constant ruled out at more than 3σ in a w_0w_a CDM model and more than 5.7σ evidence for a coupling between Dark Matter and Dark Energy in the IDE scenario. Finally, we check the robustness of our results, and we quote two additional combinations of the Hubble constant. The *ultra-conservative* estimate, $H_0 = 72.7 \pm 1.1$ km/s/Mpc at 68% CL, is obtained removing the Cepheids-SN Ia and the Time-Delay Lensing based measurements, and confirms the evidence for new physics.

Key words: cosmic background radiation – cosmological parameters – dark energy – observations

1 INTRODUCTION

The Λ CDM model provides a wonderful explanation for most of the current cosmological probes. However, its validity is questioned by the robust tensions emerged between the early and the late time Universe measurements (see Di Valentino et al. (2020a,b) for a recent overview). In particular, statistically significant is the long standing Hubble constant tension at more than 4.4σ between the H_0 value estimated by Planck in Aghanim et al. (2020b), and that measured by the SH0ES collaboration in Riess et al. (2019) (R19). The tension is made even more intriguing by the several early and late time cosmological probes (see Verde et al. (2019); Riess (2019)) in agreement, respectively, with Planck or R19, that make the systematic errors explanation more difficult, because biased always in the same direction.¹

A gigantic effort is put into resolving the Hubble constant tension, and many cosmological scenarios, in alternative or extending the Λ CDM model, have been considered. We have, for example, early modifications of the expansion history, promising because, in principle, they could solve at the same time the H_0 tension and give a lower sound horizon r_{drag} at the drag epoch (Knox & Millea (2020); Evslin et al. (2018)) as preferred by the Baryon Acoustic Oscillations (BAO) data. The Early Dark Energy (Pettorino et al. (2013); Poulin et al. (2019); Karwal & Kamionkowski (2016); Sakstein & Trodden (2020); Niedermann & Sloth (2019); Akarsu et al. (2020); Ye & Piao (2020); Agrawal et al. (2019a); Lin et al. (2019); Berghaus & Karwal (2020); Smith et al. (2020); Lucca (2020); Braglia et al.

(2020b)), and extra relativistic species at recombination (Anchordoqui & Goldberg (2012); Jacques et al. (2013); Weinberg (2013); Anchordoqui et al. (2013); Carneiro et al. (2019); Paul et al. (2019); Di Valentino et al. (2016a); Green et al. (2019); Ferreira & Notari (2018); Gelmini et al. (2019); Di Valentino et al. (2016b); Poulin et al. (2018); Baumann et al. (2016); Barenboim et al. (2017); Zeng et al. (2019); Allahverdi et al. (2014); Braglia et al. (2020a)) are the most famous models, but they can not increase the Hubble constant enough to solve the tension with R19 below 3σ (Arendse et al. (2020)). The late time modifications of the expansion history, instead, have the capability of completely solving the Hubble tension with R19 within 1σ , but leave the sound horizon unaltered, introducing a tension with the BAO data. In this category we find the phantom Dark Energy (Aghanim et al. (2020b); Yang et al. (2019c,a); Di Valentino et al. (2020d); Vagnozzi (2020); Di Valentino et al. (2020c); Keeley et al. (2019); Joudaki et al. (2017); Alestas et al. (2020)) and the Phenomenologically Emergent Dark Energy (Li & Shafieloo (2019); Pan et al. (2020); Rezaei et al. (2020); Liu & Miao (2020); Li & Shafieloo (2020); Yang et al. (2020c)). Another promising possibility is an interaction between the Dark Matter and the Dark Energy (IDE) models (Pettorino (2013); Wang et al. (2016); Kumar & Nunes (2016); Di Valentino et al. (2017); Kumar & Nunes (2017); Van De Bruck & Mifsud (2018); Yang et al. (2018b,a, 2019d); Martinelli et al. (2019); Di Valentino et al. (2020e,f); Benevento et al. (2020); Gómez-Valent et al. (2020); Lucca & Hooper (2020); Yang et al. (2020b,a, 2019b); Agrawal et al. (2019b); Anchordoqui et al. (2020b,a)), that can solve completely the Hubble constant tension. In these models there is a flux of energy between the dark matter and the dark energy, therefore, lowering the matter density, we can have a larger H_0 value for the geometrical degeneracy present in the CMB data (Di Valentino & Mena (2020)).

In this paper we combine, in an optimistic way, most of the late time

* E-mail: eleonora.di-valentino@durham.ac.uk

¹ See also Dhawan et al. (2018, 2020) for a discussion about the effect of possible systematic errors coming from dark energy model assumptions and the wavelength region of the observations.

Dataset	H_0 [km/s/Mpc]
Planck Aghanim et al. (2020b)	67.27 ± 0.60
Planck+lensing Aghanim et al. (2020b)	67.36 ± 0.54
BAO+Pantheon+BBN+ $\theta_{MC, Planck}$ Aghanim et al. (2020b)	67.9 ± 0.8
DES+BAO+BBN Abbott et al. (2018)	$67.2^{+1.2}_{-1.0}$
ACT Aiola et al. (2020)	67.9 ± 1.5
WMAP9+BAO Addison et al. (2018)	68.2 ± 0.7
SPT-SZ+BAO Addison et al. (2018)	68.3 ± 0.9
FS+BAO+BBN Philcox et al. (2020)	68.6 ± 1.1
Riess et al. (2020)	73.2 ± 1.3
Breuval et al. (2020)	73.0 ± 2.7
Riess et al. (2019)	74.03 ± 1.42
Burns et al. (2018)	73.2 ± 2.3
Freedman et al. (2012)	74.3 ± 2.1
Soltis et al. (2020)	72.1 ± 2.0
Freedman et al. (2020)	69.6 ± 1.88
Yuan et al. (2019)	72.4 ± 2.0
Jang & Lee (2017)	71.17 ± 2.50
Reid et al. (2019)	71.1 ± 1.9
Huang et al. (2019)	73.3 ± 4.0
Pesce et al. (2020)	73.9 ± 3.0
Kourkchi et al. (2020)	76.00 ± 2.55
Schombert et al. (2020)	75.10 ± 2.75
Blakeslee et al. (2021)	73.3 ± 2.5
Khetan et al. (2020)	70.5 ± 4.1
de Jaeger et al. (2020)	$75.8^{+5.2}_{-4.9}$
Wong et al. (2020)	$73.3^{+1.7}_{-1.8}$
Shajib et al. (2020)	$74.2^{+2.7}_{-3.0}$
Birrer et al. (2020)	$74.5^{+3.6}_{-3.0}$
Birrer et al. (2020)	$67.4^{+4.2}_{-3.2}$
Abbott et al. (2017)	70^{+12}_{-8}
Domínguez et al. (2019)	$67.4^{+6.0}_{-6.2}$

Table 1. H_0 values at 68% CL shown in Fig. 1, where we add in quadrature the systematic and statistic errors.

measurements of the Hubble constant together, and we use this our best H_0 estimate to constrain some of the DE models that better solve the H_0 tension, namely w CDM, w_0w_a CDM and IDE. Moreover, we test the robustness of our results using two additional Hubble constant estimates, that we will call *conservative* and *ultra-conservative*.

We introduce in Section 2 the data used in this paper and we explain the way we combine the different late time Hubble constant measurements, we present in Section 3 the Dark Energy models we consider in this work, we describe in Section 4 the method used to analyse the cosmological parameters, we discuss in Section 5 the results we obtain, and we derive in Section 6 our conclusions.

2 OBSERVATIONAL DATA

To obtain our H_0 estimates, that we will use to constrain the cosmological parameters, we combine together most of the recent late time measurements (see Fig. 1 and Table 1) with a conservative approach, taking into account that not all measurements are fully independent even between techniques. In particular, we consider the measurements based on:

(i) **Cepheids-SN Ia:** we average the H_0 measurements from Riess et al. (2020), 73.2 ± 1.3 km/s/Mpc at 68% CL, from Breuval et al. (2020) with $H_0 = 73.0 \pm 2.7$ km/s/Mpc at 68% CL, from Riess et al. (2019), $H_0 = 74.03 \pm 1.42$ km/s/Mpc at 68% CL, from Burns et al.

(2018), $H_0 = 73.2 \pm 2.3$ km/s/Mpc at 68% CL, from Freedman et al. (2012), $H_0 = 74.3 \pm 2.1$ km/s/Mpc at 68% CL, and we use the smallest error bar of the group. ² Therefore, we obtain $H_0 = 73.55 \pm 1.3$ km/s/Mpc at 68% CL for the measurements based on the Cepheids-SN Ia.

(ii) **TRGB-SN Ia:** we average the H_0 measurements from Soltis et al. (2020), 72.1 ± 2.0 km/s/Mpc at 68% CL, from Freedman et al. (2020), $H_0 = 69.6 \pm 0.8(stat) \pm 1.7(sys)$ km/s/Mpc at 68% CL, from Yuan et al. (2019), $H_0 = 72.4 \pm 2.0$ km/s/Mpc at 68% CL, from Jang & Lee (2017), $H_0 = 71.17 \pm 1.66(stat) \pm 1.87(sys)$ km/s/Mpc at 68% CL, and Reid et al. (2019), $H_0 = 71.1 \pm 1.9$ km/s/Mpc at 68% CL, and we use the smallest error bar of the group. Therefore, we obtain $H_0 = 71.27 \pm 1.88$ km/s/Mpc at 68% CL for the measurements based on the Tip of the Red Giant Branch.

(iii) **Miras-SN Ia:** we consider Huang et al. (2019), i.e. $H_0 = 73.3 \pm 4.0$ km/s/Mpc at 68% CL for measurement based on the Miras-SN Ia.

(iv) **Masers:** we consider Pesce et al. (2020), i.e. $H_0 = 73.9 \pm 3.0$ km/s/Mpc at 68% CL for the measurement based on the Masers.

(v) **Tully Fisher:** we average the H_0 measurements from Infrared Tully Fisher, Kourkchi et al. (2020), $H_0 = 76.0 \pm 1.1(stat) \pm 2.3(sys)$ km/s/Mpc at 68% CL, and from Baryonic Tully Fisher, Schombert et al. (2020), $H_0 = 75.1 \pm 2.3(stat) \pm 1.5(sys)$ km/s/Mpc at 68% CL, and we use the smallest error bar of the group. Therefore, we obtain $H_0 = 75.55 \pm 2.55$ km/s/Mpc at 68% CL for the measurements based on the Tully Fisher.

(vi) **Surface Brightness Fluctuations:** we average the H_0 measurements from Blakeslee et al. (2021), $73.3 \pm 0.7 \pm 2.4$ km/s/Mpc at 68% CL, and from Khetan et al. (2020), $H_0 = 70.50 \pm 2.37(stat) \pm 3.38(sys)$ km/s/Mpc at 68% CL, that uses SN Ia, calibrated on the SBF distance. Therefore, we obtain $H_0 = 71.9 \pm 2.5$ km/s/Mpc at 68% CL for the measurement based on the Surface Brightness Fluctuations.

(vii) **SN II:** we consider de Jaeger et al. (2020), i.e. $H_0 = 75.8^{+5.2}_{-4.9}$ km/s/Mpc at 68% CL, for the measurement based on the SN II.

(viii) **Time-delay Lensing:** we average the H_0 measurements from Wong et al. (2020) for 6 H0LiCOW lenses, $H_0 = 73.3^{+1.7}_{-1.8}$ km/s/Mpc at 68% CL, from Shajib et al. (2020) for STRIDES, $H_0 = 74.2^{+2.7}_{-3.0}$ km/s/Mpc at 68% CL, from Birrer et al. (2020) for TDCOSMO (6 H0LiCOW and 1 STRIDES lenses), $H_0 = 74.5^{+5.6}_{-6.1}$ km/s/Mpc at 68% CL, and from Birrer et al. (2020) for TDCOSMO+SLACS (adding 33 SLACS lenses without time delays), $H_0 = 67.4^{+4.2}_{-3.2}$ km/s/Mpc at 68% CL, and we use the smallest error bar of the group. Therefore, we obtain $H_0 = 72.35 \pm 1.75$ km/s/Mpc at 68% CL for the measurements based on the Time-delay Lensing. ³

² We compute the arithmetic average of these five measurements, i.e. $\frac{(73.2+73.0+74.03+73.2+74.3)}{5} = 73.55$ km/s/Mpc, but instead of quoting the error derived by the standard deviation (i.e. 0.52 km/s/Mpc in this case) we adopt a more conservative approach, preferring a larger error, i.e. the smallest error bar of the group, equal to 1.3 km/s/Mpc. We repeat the same thing for the other cases. It should be noted here that we do not adopt a weighted average because of the correlation of the measurements, but in any case this would give a stronger bound, equal to 73.59 ± 0.78 km/s/Mpc.

³ The results from Wong et al. (2020) for 6 H0LiCOW lenses and from Shajib et al. (2020) for STRIDES were obtained assuming the deflector mass density profiles by either a power-law or stars (constant mass-to-light ratio) plus standard dark matter halos, while the updated analysis in TDCOSMO IV does not rely on these assumptions on the radial density profiles, encodes the mass-sheet degeneracy in the inference and adds external lenses from the SLACS to provide quantitative constraints on the radial density profiles, providing a solid foundation of agnostic assumptions.

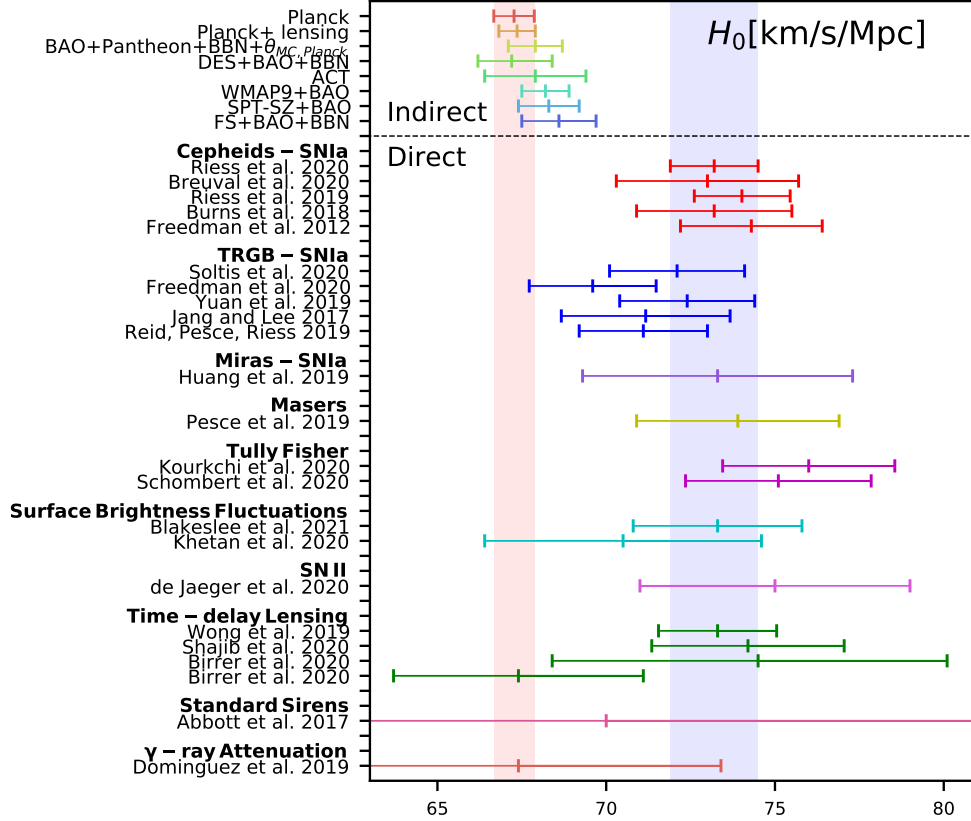


Figure 1. Some of the Hubble constant measurements present in the literature: see Table 1 for the values. Those averaged to obtain our H_0 estimates are instead listed in Section 4.

(ix) **Gravitational Wave Standard Sirens:** we consider [Abbott et al. \(2017\)](#), i.e. $H_0 = 70^{+12}_{-8}$ km/s/Mpc at 68% CL, for the measurement based on the Standard Sirens.

(x) **γ -ray Attenuation:** we consider [Domínguez et al. \(2019\)](#), i.e. $H_0 = 67.4^{+6.0}_{-6.2}$ km/s/Mpc at 68% CL, for the measurement based on the γ -ray Attenuation.

At this point we consider a weighted average of the 10 estimates listed above, obtaining our best H_0 estimate, i.e. $H_0 = 72.94 \pm 0.75$ km/s/Mpc at 68% CL, in agreement with [Verde et al. \(2019\)](#). Computing the average over different measurements, made by different teams with different methods, can in principle ensure a more reliable H_0 estimate, perhaps canceling possible biases, so we will call our best estimate *optimistic*. We notice here that we can safely add all the datasets together because all of them are in agreement within 2σ . However, there is some overlap between the data (i),(ii), (iii), i.e. Cepheids, TRGB and Miras respectively, and SBF from [Khetan et al. \(2020\)](#) that use the same SN Ia ladders, and a more accurate analysis should account for their covariance. Therefore, in order to check the robustness and consistency of our optimistic estimate, we do a "jackknife test" of the results, producing 10 averages with each leaving out a different dataset, in Table 2, and 45 averages leaving

out every combination of two, in Table 3. In particular, the exclusion of one measurement changes the H_0 estimate from the minimum mean value $H_0 = 72.63$ km/s/Mpc to the maximum mean value $H_0 = 73.25$ km/s/Mpc (see Table 2), while the exclusion of two measurements changes the H_0 estimate from minimum mean value $H_0 = 72.19$ km/s/Mpc to the maximum mean value $H_0 = 73.51$ km/s/Mpc (see Table 3). The robustness test shows that the exclusion of one or two of the listed measurements doesn't change quantitatively our conclusions on the DE models.

Regarding the correlation between the measurements (i),(ii) and (iii) (Cepheids, TRGB and Miras respectively)⁴ we can see from Table 3 that considering only one of them per time does not change significantly our optimistic estimate. In particular we find that removing (i) and (ii) we have $H_0 = 73.1 \pm 1.1$ km/s/Mpc at 68% CL, removing (i) and (iii) we have $H_0 = 72.59 \pm 0.95$ km/s/Mpc at 68% CL, and removing (ii) and (iii) we have $H_0 = 73.25 \pm 0.84$ km/s/Mpc at 68% CL. For this reason, we make use in the analysis of the DE

⁴ The measurement from [Khetan et al. \(2020\)](#) based on SBF-SN has instead a relative larger uncertainty and is averaged with [Blakeslee et al. \(2021\)](#), that has the galaxies directly in the Hubble flow.

H_0 mean	H_0 error	excluded
72.62699	0.9233376	1
73.25471	0.8215147	2
72.92314	0.7664772	3
72.87175	0.7776620	4
72.68698	0.7878957	5
73.03983	0.7894195	6
72.87141	0.7612871	7
73.06965	0.8338738	8
72.95322	0.7549235	9
73.02211	0.7585800	10

Table 2. Robustness test of the results, excluding the measurement indicated in the last column.

models of an additional *conservative* estimate of H_0 from the Table 2 excluding one dataset and taking the result with the largest error bar, i.e. $H_0 = 72.63 \pm 0.92$ km/s/Mpc at 68% CL without the Cepheids-SN Ia based measurement. And we consider an *ultra-conservative* estimate from the Table 3 excluding two datasets and taking the result with the largest error bar, i.e. $H_0 = 72.7 \pm 1.1$ km/s/Mpc at 68% CL, without also the Time-Delay Lensing based measurement.

The cosmological constraints on the parameters of the models we are analysing in this paper are then obtained, making use of the following data:

- **Planck:** for this dataset we consider the latest temperature and polarization Cosmic Microwave Background (CMB) power spectra data as measured by the final 2018 Planck legacy release (Aghanim et al. (2020b,a)).
- **ACT+WMAP:** we include this dataset combination as in Ref. Aiola et al. (2020), as a crosscheck of the results, making use of the latest temperature and polarization CMB power spectra data as measured by ACT (Aiola et al. (2020)), and combined with WMAP9 (Bennett et al. (2013)) and a τ prior.
- **$optH_0$:** we use a Gaussian prior on the Hubble constant as obtained by combining together, in an optimistic way, most of the late time measurement, i.e. $H_0 = 72.94 \pm 0.75$ km/s/Mpc at 68% CL. Moreover, we compare our results with those obtained using the conservative prior $H_0 = 72.63 \pm 0.92$ km/s/Mpc at 68% CL, i.e. **$consH_0$** , and the ultra-conservative prior $H_0 = 72.7 \pm 1.1$ km/s/Mpc at 68% CL, i.e. **$ultraH_0$** .

3 MODELS

Even if a Λ CDM model provides a beautiful description of the available cosmological data, we can not ignore the many H_0 measurements at late time providing a larger value for the Hubble constant. Our best optimistic estimate of $H_0 = 72.94 \pm 0.75$ km/s/Mpc at 68 % CL is, in fact, at 5.9σ of disagreement with the Planck estimate in a Λ CDM model. Moreover, our H_0 estimate increases also the tension with the early time solutions, therefore making the late time solutions more appealing.

Actually, it is well known that BAO, combined with high- z SNe data, constrain the product $r_{\text{drag}}H_0$, and combining them with either CMB or R19 leaves the other choice in tension, so the early time solutions are preferred because can modify both r_{drag} and H_0 in the right directions. However, we have chosen here to explore the most powerful extensions in solving the Hubble tension, without considering BAO and high- z SNe data. Actually, doing so may offer insight

H_0 mean	H_0 error	excluded	excluded
73.05838	1.059989	1	2
72.58911	0.9489663	1	3
72.49379	0.9704452	1	4
72.18593	0.9905548	1	5
72.74182	0.9935880	1	6
72.51725	0.9391693	1	7
72.73386	1.086945	1	8
72.64958	0.9272990	1	9
72.74957	0.9341007	1	10
73.25271	0.8394086	2	3
73.20239	0.8541644	2	4
72.98889	0.8677809	2	5
73.41869	0.8698181	2	6
73.18552	0.8326054	2	7
73.51043	0.9304035	2	8
73.27682	0.8243009	2	9
73.36285	0.8290675	2	10
72.85492	0.7927890	3	4
72.66224	0.8036401	3	5
73.02929	0.8052573	3	6
72.85530	0.7754612	3	7
73.05918	0.8526064	3	8
72.94041	0.7687386	3	9
73.01174	0.7726005	3	10
72.59712	0.8165602	4	5
72.97585	0.8182568	4	6
72.80062	0.7870499	4	7
73.00013	0.7800242	4	9
72.96215	0.7840596	4	10
72.77377	0.8302036	5	6
72.60931	0.7976639	5	7
72.77266	0.8823864	5	8
72.70377	0.7903527	5	9
72.77669	0.7945514	5	10
72.97070	0.7992452	6	7
73.21607	0.8845285	6	8
73.05890	0.7918909	6	9
73.13590	0.7961143	6	10
72.99312	0.8454798	7	8
72.88815	0.7635028	7	9
72.95798	0.7672859	7	10
73.09115	0.8367882	8	9
73.17762	0.8417761	8	10
73.03960	0.7607720	9	10

Table 3. Robustness test of the results, excluding the measurements indicated in the last 2 columns.

on some of the most famous DE models explored in the literature, focusing on just H_0 and neglecting for the moment additional datasets, that can bring further systematic errors in the general picture.

Therefore, in this work we analyze three different models, famous for their ability to solve the Hubble constant tension within 2σ , so in good agreement with R19 and with our best optimistic estimate of H_0 , as well as our conservative and ultra-conservative H_0 values.

First of all, we consider the w CDM model, where instead of a cosmological constant $w = -1$ there is a dark energy equation of state of the form $w = P/\rho$, where P and ρ are the dark energy pressure and dark energy density respectively, and w is a free parameter time independent.

As a second scenario, we consider the w_0w_a CDM model, where there is a dark energy equation of state time dependent following the parametrization independently proposed by Chevallier & Polarski

Parameter	prior
$\Omega_b h^2$	[0.005, 0.1]
$\Omega_c h^2$	[0.001, 0.99]
$100\theta_{MC}$	[0.5, 10]
τ	[0.01, 0.8]
n_s	[0.7, 1.3]
$\log[10^{10} A_s]$	[1.7, 5.0]
w_0	[-3, 1]
w_a	[-3, 2]
ξ	[-1, 0]

Table 4. Flat priors on the cosmological parameters varied in this work.

(2001) and Linder (2003), also known as CPL:

$$w_x(a) = w_0 + w_a(1 - a). \quad (1)$$

In this parametrization, the dark energy equation of state parameter w_a gives the evolution of $w(a)$ with redshift, while w_0 gives the value of the dark energy equation of state today.

Finally, we consider an interacting dark energy scenario IDE, i.e. a class of models where the Dark Matter and Dark Energy continuity equations are described by Valiviita et al. (2008); Gavela et al. (2009); Honorez et al. (2010); del Campo et al. (2009); Gavela et al. (2010); Di Valentino et al. (2020e,f):

$$\dot{\rho}_c + 3\mathcal{H}\rho_c = Q, \quad (2)$$

$$\dot{\rho}_x + 3\mathcal{H}(1+w)\rho_x = -Q. \quad (3)$$

In these equations, the dot refer to the derivative with respect to the conformal time τ , ρ_c is the dark matter energy density, \mathcal{H} is the conformal expansion rate of the universe, ρ_x is dark energy density. In our analysis, we assume a constant dark energy equation of state $w = -0.999$, and a coupling function Q given by:

$$Q = \xi\mathcal{H}\rho_x, \quad (4)$$

where ξ is a negative dimensionless parameter, describing the coupling between the dark matter and the dark energy fluids.

4 METHODOLOGY

We analyse three different baseline models, namely w CDM, w_0w_a CDM and IDE described in Section 3. The common 6 cosmological parameters of the models considered in this work are the baryon energy density $\Omega_b h^2$, the cold dark matter energy density $\Omega_c h^2$, the ratio between the sound horizon and the angular diameter distance at decoupling θ_{MC} , the reionization optical depth τ , the amplitude of the scalar primordial power spectrum A_s , the spectral index n_s . The specific parameters of the cosmological scenario analysed with the data, are instead the constant Dark Energy equation of state w for the w CDM model, the 2 parameters of the redshift dependent Dark Energy equation of state w_0, w_a for the w_0w_a CDM model, and the dimensionless coupling ξ for the IDE model. We adopt on the parameters the flat priors listed in Table 4.

For the data analysis, we make use of the publicly available MCMC code CosmoMC (Lewis & Bridle (2002)) (see <http://cosmologist.info/cosmomc/>), also modified to implement the IDE model. This code implements an efficient sampling of the posterior distribution using the fast/slow parameter decorrelations (Lewis (2013)), and makes use of a convergence diagnostic based on the Gelman-Rubin statistics (Gelman & Rubin (1992)).

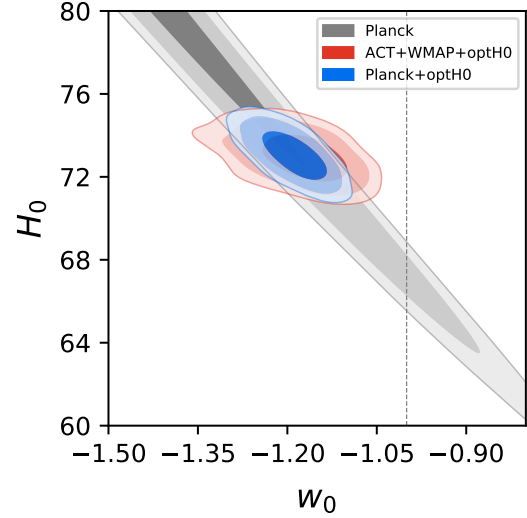


Figure 2. 68%, 95% and 99% contour plots for the w CDM model in the plane (w_0, H_0) . We can see the evidence for a phantom Dark Energy equation of state at more than 5σ for Planck+*optH0*, and at more than 3σ for ACT+WMAP+*optH0*.

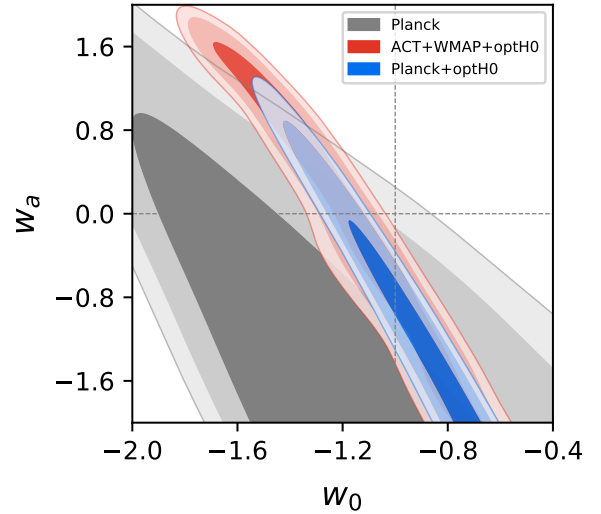


Figure 3. 68%, 95% and 99% contour plots for the w_0w_a CDM model in the plane (w_0, w_a) . We can see that both the dataset combinations, Planck+*optH0* and ACT+WMAP+*optH0*, are ruling out a cosmological constant, i.e. the point $(w_0 = -1, w_a = 0)$, at many standard deviations with a large statistical significance.

5 RESULTS

We present in Table 5 the 68% CL constraints on the cosmological parameters of the DE models explored in this work (w CDM, w_0w_a CDM and IDE) obtained combining Planck with our optimistic H_0 prior, i.e. $H_0 = 72.94 \pm 0.75$ km/s/Mpc at 68% CL, presented in Section 4. We show, instead, in Table 7 the bounds on the cosmological models w CDM and w_0w_a CDM we find combining ACT+WMAP and our optimistic H_0 prior. We remind here that we can combine these measurements safely because in good agreement with our optimistic H_0 prior within these cosmological scenarios.

[tb]

Table 5. 68% CL constraints for the w CDM, w_0w_a CDM and IDE scenarios explored in this work, for Planck and Planck+ $optH_0$.

Parameters	wCDM	wCDM	w_0w_a CDM	w_0w_a CDM	IDE	IDE
	Planck	Planck + $optH_0$	Planck	Planck + $optH_0$	Planck	Planck + $optH_0$
$\Omega_b h^2$	0.02240 ± 0.00015	0.02238 ± 0.00015	0.02240 ± 0.00015	0.02240 ± 0.00015	0.02239 ± 0.000015	0.02238 ± 0.000014
$\Omega_c h^2$	0.1199 ± 0.0014	$0.1201^{+0.0014}_{-0.0015}$	0.1198 ± 0.0014	0.1198 ± 0.0014	< 0.0634	$0.046^{+0.014}_{-0.012}$
$100\theta_{MC}$	1.04093 ± 0.00031	1.04091 ± 0.00031	1.04094 ± 0.00031	1.04092 ± 0.00031	$1.0458^{+0.0033}_{-0.0021}$	$1.0458^{+0.0009}_{-0.0012}$
τ	0.0540 ± 0.0079	0.0536 ± 0.0080	$0.0541^{+0.0073}_{-0.0084}$	0.0544 ± 0.0081	0.0541 ± 0.0076	0.0540 ± 0.0076
n_s	0.9654 ± 0.0044	$0.9649^{+0.0052}_{-0.0046}$	0.9657 ± 0.0043	0.9655 ± 0.0043	0.9655 ± 0.0043	0.9652 ± 0.0042
$\ln(10^{10} A_s)$	3.044 ± 0.016	3.043 ± 0.016	3.044 ± 0.017	3.044 ± 0.017	3.044 ± 0.0016	3.044 ± 0.0016
ξ	0	0	0	0	$-0.54^{+0.12}_{-0.28}$	$-0.57^{+0.10}_{-0.09}$
w_0	$-1.58^{+0.16}_{-0.35}$	$-1.187^{+0.038}_{-0.030}$	$-1.25^{+0.40}_{-0.56}$	$-0.83^{+0.29}_{-0.17}$	-0.999	-0.999
w_a	0	0	< -0.646	< -1.05	0	0
H_0 [km/s/Mpc]	> 82.5	72.97 ± 0.75	> 79.5	72.96 ± 0.74	$72.8^{+3.0}_{-1.5}$	73.04 ± 0.74
S_8	$0.778^{+0.023}_{-0.036}$	0.817 ± 0.015	$0.786^{+0.026}_{-0.044}$	0.819 ± 0.015	$1.30^{+0.17}_{-0.44}$	$1.24^{+0.09}_{-0.18}$
r_d [Mpc]	147.08 ± 0.30	147.05 ± 0.31	147.10 ± 0.30	147.11 ± 0.30	147.08 ± 0.30	147.06 ± 0.29

[tb]

Table 6. 68% CL constraints for the w CDM, w_0w_a CDM and IDE scenarios explored in this work, for Planck+ $consH_0$ and Planck+ $ultraH_0$.

Parameters	wCDM	wCDM	w_0w_a CDM	w_0w_a CDM	IDE	IDE
	Planck + $consH_0$	Planck + $ultraH_0$	Planck + $consH_0$	Planck + $ultraH_0$	Planck + $consH_0$	Planck + $ultraH_0$
ξ	0	0	0	0	-0.55 ± 0.11	-0.56 ± 0.12
w_0	$-1.178^{+0.040}_{-0.033}$	$-1.182^{+0.045}_{-0.038}$	$-0.82^{+0.29}_{-0.17}$	$-0.82^{+0.29}_{-0.17}$	-0.999	-0.999
w_a	0	0	< -1.04	< -1.05	0	0
H_0 [km/s/Mpc]	72.69 ± 0.91	72.8 ± 1.1	72.67 ± 0.92	72.8 ± 1.1	72.79 ± 0.91	72.9 ± 1.1
S_8	0.818 ± 0.015	0.818 ± 0.015	0.820 ± 0.015	0.820 ± 0.015	$1.21^{+0.09}_{-0.19}$	$1.23^{+0.10}_{-0.22}$
r_d [Mpc]	147.05 ± 0.30	147.05 ± 0.30	147.11 ± 0.30	147.11 ± 0.31	147.06 ± 0.29	147.06 ± 0.29

[tb]

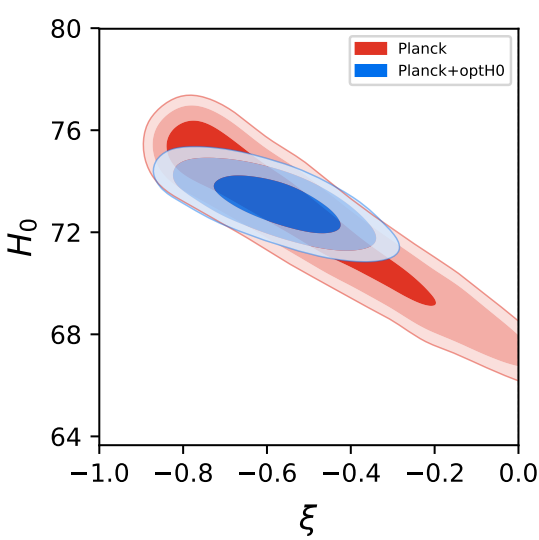
Table 7. 68% CL constraints for the w CDM and w_0w_a CDM scenarios explored in this work, for ACT+WMAP and ACT+WMAP+ $optH_0$.

Parameters	wCDM	wCDM	w_0w_a CDM	w_0w_a CDM
	ACT + WMAP	ACT + WMAP + $optH_0$	ACT + WMAP	ACT + WMAP + $optH_0$
$\Omega_b h^2$	0.02238 ± 0.00020	0.02239 ± 0.00020	0.02238 ± 0.00021	0.02237 ± 0.00021
$\Omega_c h^2$	0.1202 ± 0.0027	0.1200 ± 0.0025	0.1203 ± 0.0028	$0.1203^{+0.0026}_{-0.0029}$
$100\theta_{MC}$	1.04167 ± 0.00064	1.04172 ± 0.00066	1.04168 ± 0.00065	$1.04171^{+0.00070}_{-0.00064}$
τ	0.062 ± 0.013	0.062 ± 0.013	0.061 ± 0.013	0.061 ± 0.013
n_s	0.9727 ± 0.0063	0.9730 ± 0.0059	0.9727 ± 0.0064	0.9725 ± 0.0062
$\ln(10^{10} A_s)$	3.067 ± 0.024	3.066 ± 0.024	3.065 ± 0.024	3.064 ± 0.024
w_0	$-1.12^{+0.56}_{-0.32}$	$-1.172^{+0.052}_{-0.040}$	$-0.83^{+0.69}_{-0.83}$	-1.07 ± 0.33
w_a	0	0	< -0.158	< 0.327
H_0 [km/s/Mpc]	72^{+9}_{-20}	72.87 ± 0.73	70^{+10}_{-20}	72.90 ± 0.75
S_8	$0.828^{+0.049}_{-0.043}$	0.827 ± 0.025	0.836 ± 0.051	0.827 ± 0.028
r_d [Mpc]	147.03 ± 0.63	147.07 ± 0.61	147.00 ± 0.66	$147.02^{+0.68}_{-0.61}$

[tb]

Table 8. 68% CL constraints for the w CDM and w_0w_a CDM scenarios explored in this work, for ACT+WMAP+*cons* H_0 and ACT+WMAP+*ultra* H_0 .

Parameters	wCDM	wCDM	w_0w_a CDM	w_0w_a CDM
	ACT + WMAP + <i>cons</i> H_0	ACT + WMAP + <i>ultra</i> H_0	ACT + WMAP + <i>cons</i> H_0	ACT + WMAP + <i>ultra</i> H_0
w_0	$-1.163^{+0.053}_{-0.043}$	$-1.165^{+0.056}_{-0.046}$	$-1.06^{+0.38}_{-0.34}$	$-1.05^{+0.39}_{-0.33}$
w_a	0	0	$-0.5^{+1.9}_{-1.3}$	$-0.6^{+1.9}_{-1.3}$
H_0 [km/s/Mpc]	72.58 ± 0.88	72.6 ± 1.1	72.58 ± 0.92	72.6 ± 1.1
S_8	0.828 ± 0.026	0.828 ± 0.026	0.829 ± 0.028	0.828 ± 0.028
r_d [Mpc]	147.06 ± 0.61	147.07 ± 0.61	$147.01^{+0.68}_{-0.62}$	147.01 ± 0.67


Figure 4. 68%, 95% and 99% contour plots for the IDE model in the plane (ξ, H_0) . We see for Planck+*opt* H_0 a strong evidence for an interaction between the dark energy and the dark matter at more than 6σ .

The w CDM cosmological constraints are reported in the first two columns of Table 5 and Table 7. We can see a good agreement between Planck and ACT+WMAP, but with Planck preferring a larger Hubble constant and a more phantom dark energy equation of state than ACT+WMAP. In particular, while $H_0 > 82.5$ km/s/Mpc at 68% CL for Planck, therefore in agreement with our optimistic H_0 estimate at 95% CL, ACT+WMAP finds $H_0 = 72^{+9}_{-20}$ km/s/Mpc at 68% CL, i.e. in agreement within 1σ with our *opt* H_0 prior. Combining these CMB datasets with our optimistic H_0 , we find instead a perfect agreement between the two dataset combinations, Planck based and ACT based, removing the main differences. Planck+*opt* H_0 gives, in fact, an evidence for a phantom Dark Energy equation of state at more than 4.9σ , i.e. $w = -1.187^{+0.038}_{-0.030}$ at 68% CL, in agreement with ACT+WMAP+*opt* H_0 , that finds $w = -1.172^{+0.052}_{-0.040}$ at 68% CL, ruling out the cosmological constant at more than 3.3σ . The correlation between w and H_0 can be seen in Fig. 2, as well as the strong evidence for a phantom dark energy coming from both, Planck+*opt* H_0 and ACT+WMAP+*opt* H_0 . To test the robustness of our results, we make use of our conservative H_0 estimate $H_0 = 72.63 \pm 0.92$ km/s/Mpc at 68% CL, obtaining $w = -1.178^{+0.040}_{-0.033}$ at 68% CL for Planck+*cons* H_0 , corre-

sponding to the first column of Table 6, and $w = -1.163^{+0.053}_{-0.043}$ at 68% CL for ACT+WMAP+*cons* H_0 , corresponding to the first column of Table 8. Additionally, if we move to our ultra-conservative H_0 estimate, $H_0 = 72.7 \pm 1.1$ km/s/Mpc at 68% CL, we obtain $w = -1.182^{+0.045}_{-0.038}$ at 68% CL for Planck+*ultra* H_0 , corresponding to the second column of Table 6, and $w = -1.165^{+0.056}_{-0.046}$ at 68% CL for ACT+WMAP+*ultra* H_0 , corresponding to the second column of Table 8. Therefore, we are ruling out the cosmological constant at more than 3σ in all the cases.

The constraints on the cosmological parameters of the w_0w_a CDM scenario are shown in the columns 3 and 4 of Table 5 and Table 7. Also in this case, we have a good agreement between Planck and ACT+WMAP, with Planck preferring a larger H_0 value than ACT+WMAP. In particular, Planck gives $H_0 > 79.5$ km/s/Mpc at 68% CL, in agreement with our H_0 estimates at 95% CL, while ACT+WMAP prefers $H_0 = 70^{+10}_{-20}$ km/s/Mpc at 68% CL, in agreement within 1σ with our *opt* H_0 prior. If we now combine these two dataset combinations with our optimistic H_0 estimate, Planck+*opt* H_0 gives $w_0 = -0.83^{+0.29}_{-0.17}$ and $w_a < -1.05$ at 68% CL, and ACT+WMAP+*opt* H_0 finds $w_0 = -1.07 \pm 0.33$ and $w_a < 0.327$ at 68% CL. In Fig. 3, we can see as both, Planck+*opt* H_0 and ACT+WMAP+*opt* H_0 , are ruling out a cosmological constant, i.e. the point $(w_0 = -1, w_a = 0)$, at more than 3 standard deviations. To check the robustness of our constraints, we make use of our conservative H_0 estimate obtaining $w_0 = -0.82^{+0.29}_{-0.17}$ and $w_a < -1.04$ at 68% CL for Planck+*cons* H_0 , in Table 6, and $w_0 = -1.06^{+0.38}_{-0.34}$ and $w_a = -0.5^{+1.9}_{-1.3}$ at 68% CL for ACT+WMAP+*cons* H_0 in Table 8. Moreover, for our ultra-conservative H_0 estimate, we have $w_0 = -0.82^{+0.29}_{-0.17}$ and $w_a < -1.05$ at 68% CL for Planck+*ultra* H_0 (Table 6) and $w_0 = -1.05^{+0.39}_{-0.33}$ and $w_a = -0.6^{+1.9}_{-1.3}$ at 68% CL for ACT+WMAP+*ultra* H_0 (Table 8). In all the cases we are ruling out the cosmological constant in the plane (w_0, w_a) at more than 3σ .

The constraints for the IDE scenario are shown in the columns 5 and 6 of Table 5. In this model we have a suspicious evidence for a coupling between the dark matter and the dark energy, possibly due to the correlation of the parameters, as shown in Di Valentino & Mena (2020), for Planck alone. In particular, for this model, Planck gives $H_0 = 72.8^{+3.0}_{-1.5}$ km/s/Mpc at 68% CL, in agreement with our optimistic H_0 estimate at 68% CL. If we now combine this dataset with our optimistic H_0 prior, we break the degeneracy between the parameters, obtaining for Planck+*opt* H_0 a coupling $\xi = -0.57^{+0.10}_{-0.09}$ at 68% CL, i.e. a strong evidence for an interaction between the dark energy and the dark matter at more than 5.7σ , as we can see also in Fig. 4. It is worthwhile to note that making use of the our

conservative H_0 prior we have $\xi = -0.55 \pm 0.11$ at 68% CL, and of our ultra-conservative H_0 prior we have $\xi = -0.56 \pm 0.12$ at 68% CL, reducing the evidence for the coupling at 5σ and 4.7σ respectively, corresponding to the last two columns of Table 6.

6 CONCLUSIONS

In this paper we study the impact of the Hubble Constant H_0 late time measurements on the Dark Energy sector. Firstly, we combine some of the latest H_0 measurements, testing the consistency and robustness of the results excluding one, or two, different measurements per time. Then, we define our best optimistic H_0 estimate, that is $H_0 = 72.94 \pm 0.75$ km/s/Mpc at 68% CL, obtained averaging over different measurements, made by different teams with different methods, in order to guarantee a more reliable H_0 estimate, possibly canceling likely biases. Finally, we evaluate the impact of this H_0 prior on extended Dark Energy cosmologies, in particular w CDM, with a constant dark energy equation of state, $w_0 w_a$ CDM, with a varying with redshift dark energy equation of state, and an IDE scenario, where there is an interaction between dark matter and dark energy.

We find for w CDM that a combination of Planck+*opt* H_0 gives an evidence for a phantom Dark Energy equation of state at more than 4.9σ , i.e. $w = -1.187^{+0.038}_{-0.030}$ at 68% CL, and this result is supported by ACT+WMAP+*opt* H_0 that finds $w < -1$ at more than 3σ , i.e. $w = -1.172^{+0.052}_{-0.040}$ at 68% CL.

We find for $w_0 w_a$ CDM that both the dataset combinations, Planck+*opt* H_0 and ACT+WMAP+*opt* H_0 , are ruling out a cosmological constant, i.e. the point ($w_0 = -1, w_a = 0$), at more than 3σ .

We see for Planck+*opt* H_0 a coupling $\xi = -0.57^{+0.10}_{-0.09}$ at 68% CL, i.e. a strong evidence for an interaction between the dark energy and the dark matter at more than 5.7σ .

Finally, if we check the robustness of our conclusions making use of a conservative or ultra-conservative H_0 priors, we find that these results are confirmed. We remind here that these DE models are in any case in tension with BAO and high- z SNe data.

ACKNOWLEDGEMENTS

The author thanks Adam Riess for explanations regarding differences in Hubble constant measurements, and Simon Birrer for those based on the Time-delay Lensing. In addition, the author thanks Alessandro Melchiorri and Olga Mena for useful discussions. The author acknowledges the support of the Addison-Wheeler Fellowship awarded by the Institute of Advanced Study at Durham University.

DATA AVAILABILITY

We used current publicly available cosmological probes, as listed in the section "Observational Data".

REFERENCES

Abbott B. P., et al., 2017, *Nature*, 551, 85
 Abbott T., et al., 2018, *Mon. Not. Roy. Astron. Soc.*, 480, 3879
 Addison G., Watts D., Bennett C., Halpern M., Hinshaw G., Weiland J., 2018, *Astrophys. J.*, 853, 119
 Aghanim N., et al., 2020a, *Astron. Astrophys.*, 641, A5
 Aghanim N., et al., 2020b, *Astron. Astrophys.*, 641, A6

Agrawal P., Obied G., Vafa C., 2019b, arXiv:1906.08261
 Agrawal P., Cyr-Racine F.-Y., Pinner D., Randall L., 2019a, arXiv:1904.01016
 Aiola S., et al., 2020, arXiv:2007.07288
 Akarsu Ö., Barrow J. D., Escamilla L. A., Vazquez J. A., 2020, *Phys. Rev. D*, 101, 063528
 Alestas G., Kazantzidis L., Perivolaropoulos L., 2020, *Phys. Rev. D*, 101, 123516
 Allahverdi R., Cicoli M., Dutta B., Sinha K., 2014, *JCAP*, 10, 002
 Anchordoqui L. A., Goldberg H., 2012, *Phys. Rev. Lett.*, 108, 081805
 Anchordoqui L. A., Goldberg H., Steigman G., 2013, *Phys. Lett. B*, 718, 1162
 Anchordoqui L. A., Antoniadis I., Lüst D., Soriano J. F., 2020a, arXiv:2005.10075
 Anchordoqui L. A., Antoniadis I., Lüst D., Soriano J. F., Taylor T. R., 2020b, *Phys. Rev. D*, 101, 083532
 Arendse N., et al., 2020, *Astron. Astrophys.*, 639, A57
 Barenboim G., Kinney W. H., Park W.-I., 2017, *Eur. Phys. J. C*, 77, 590
 Baumann D., Green D., Wallisch B., 2016, *Phys. Rev. Lett.*, 117, 171301
 Benevento G., Hu W., Raveri M., 2020, *Phys. Rev. D*, 101, 103517
 Bennett C., et al., 2013, *Astrophys. J. Suppl.*, 208, 20
 Berghaus K. V., Karwal T., 2020, *Phys. Rev. D*, 101, 083537
 Birrer S., et al., 2020, *Astron. Astrophys.*, 643, A165
 Blakeslee J. P., Jensen J. B., Ma C.-P., Milne P. A., Greene J. E., 2021, arXiv:2101.02221
 Braglia M., Ballardini M., Emond W. T., Finelli F., Gumrukcuoglu A. E., Koyama K., Paoletti D., 2020a, *Phys. Rev. D*, 102, 023529
 Braglia M., Emond W. T., Finelli F., Gumrukcuoglu A. E., Koyama K., 2020b, *Phys. Rev. D*, 102, 083513
 Breuval L., et al., 2020, *Astron. Astrophys.*, 643, A115
 Burns C. R., et al., 2018, *Astrophys. J.*, 869, 56
 Carneiro S., de Holanda P. C., Pigozzo C., Sobreira F., 2019, *Phys. Rev.*, D100, 023505
 Chevallier M., Polarski D., 2001, *Int. J. Mod. Phys.*, D10, 213
 Dhawan S., Jha S. W., Leibundgut B., 2018, *Astron. Astrophys.*, 609, A72
 Dhawan S., Brout D., Scolnic D., Goobar A., Riess A., Miranda V., 2020, *Astrophys. J.*, 894, 54
 Di Valentino E., Mena O., 2020, *MNRAS-L*
 Di Valentino E., Giusarma E., Mena O., Melchiorri A., Silk J., 2016a, *Phys. Rev.*, D93, 083527
 Di Valentino E., Giusarma E., Lattanzi M., Mena O., Melchiorri A., Silk J., 2016b, *Phys. Lett.*, B752, 182
 Di Valentino E., Melchiorri A., Mena O., 2017, *Phys. Rev.*, D96, 043503
 Di Valentino E., et al., 2020a, arXiv:2008.11284
 Di Valentino E., et al., 2020b, arXiv:2008.11285
 Di Valentino E., Mukherjee A., Sen A. A., 2020c, arXiv:2005.12587
 Di Valentino E., Melchiorri A., Silk J., 2020d, *JCAP*, 01, 013
 Di Valentino E., Melchiorri A., Mena O., Vagnozzi S., 2020e, *Phys. Dark Univ.*, 30, 100666
 Di Valentino E., Melchiorri A., Mena O., Vagnozzi S., 2020f, *Phys. Rev. D*, 101, 063502
 Domínguez A., et al., 2019, arXiv:1903.12097
 Evslin J., Sen A. A., Ruchika 2018, *Phys. Rev. D*, 97, 103511
 Ferreira R. Z., Notari A., 2018, *Phys. Rev. Lett.*, 120, 191301
 Freedman W. L., Madore B. F., Scowcroft V., Burns C., Monson A., Persson S. E., Seibert M., Rigby J., 2012, *The Astrophysical Journal*, 758, 24
 Freedman W. L., et al., 2020, arXiv:2002.01550
 Gavela M., Hernandez D., Lopez Honorez L., Mena O., Rigolin S., 2009, *JCAP*, 07, 034
 Gavela M., Lopez Honorez L., Mena O., Rigolin S., 2010, *JCAP*, 11, 044
 Gelman A., Rubin D. B., 1992, *Statist. Sci.*, 7, 457
 Gelmini G. B., Kusenko A., Takhistov V., 2019, arXiv:1906.10136
 Green D., et al., 2019, *Bull. Am. Astron. Soc.*, 51, 159
 Gómez-Valent A., Pettorino V., Amendola L., 2020, *Phys. Rev. D*, 101, 123513
 Honorez L. L., Reid B. A., Mena O., Verde L., Jimenez R., 2010, *Journal of Cosmology and Astroparticle Physics*, 2010, 029–029
 Huang C. D., et al., 2019, *ApJ*
 Jacques T. D., Krauss L. M., Lunardini C., 2013, *Phys. Rev. D*, 87, 083515
 Jang I. S., Lee M. G., 2017, *Astrophys. J.*, 836, 74
 Joudaki S., et al., 2017, *Mon. Not. Roy. Astron. Soc.*, 471, 1259

- Karwal T., Kamionkowski M., 2016, *Phys. Rev. D*, 94, 103523
- Keeley R. E., Joudaki S., Kaplinghat M., Kirkby D., 2019, *JCAP*, 12, 035
- Khetan N., et al., 2020, arXiv:2008.07754
- Knox L., Millea M., 2020, *Phys. Rev. D*, 101, 043533
- Kourkchi E., Tully R. B., Anand G. S., Courtois H. M., Dupuy A., Neill J. D., Rizzi L., Seibert M., 2020, *Astrophys. J.*, 896, 3
- Kumar S., Nunes R. C., 2016, *Phys. Rev.*, D94, 123511
- Kumar S., Nunes R. C., 2017, *Phys. Rev.*, D96, 103511
- Lewis A., 2013, *Phys. Rev. D*, 87, 103529
- Lewis A., Bridle S., 2002, *Phys. Rev. D*, 66, 103511
- Li X., Shafieloo A., 2019, *Astrophys. J. Lett.*, 883, L3
- Li X., Shafieloo A., 2020, *Astrophys. J.*, 902, 58
- Lin M.-X., Benevento G., Hu W., Raveri M., 2019, *Phys. Rev. D*, 100, 063542
- Linder E. V., 2003, *Phys. Rev. Lett.*, 90, 091301
- Liu Z., Miao H., 2020, *Int. J. Mod. Phys. D*, 29, 2050088
- Lucca M., 2020, *Phys. Lett. B*, 810, 135791
- Lucca M., Hooper D. C., 2020, *Phys. Rev. D*, 102, 123502
- Martinelli M., Hogg N. B., Peirone S., Bruni M., Wands D., 2019, *Mon. Not. Roy. Astron. Soc.*, 488, 3423
- Niedermann F., Sloth M. S., 2019, arXiv:1910.10739
- Pan S., Yang W., Di Valentino E., Shafieloo A., Chakraborty S., 2020, *JCAP*, 06, 062
- Paul A., Ghoshal A., Chatterjee A., Pal S., 2019, *Eur. Phys. J.*, C79, 818
- Pesce D., et al., 2020, *Astrophys. J. Lett.*, 891, L1
- Pettorino V., 2013, *Phys. Rev. D*, 88, 063519
- Pettorino V., Amendola L., Wetterich C., 2013, *Phys. Rev. D*, 87, 083009
- Philcox O. H., Ivanov M. M., Simonović M., Zaldarriaga M., 2020, *JCAP*, 05, 032
- Poulin V., Smith T. L., Grin D., Karwal T., Kamionkowski M., 2018, *Phys. Rev. D*, 98, 083525
- Poulin V., Smith T. L., Karwal T., Kamionkowski M., 2019, *Phys. Rev. Lett.*, 122, 221301
- Reid M., Pesce D., Riess A., 2019, *Astrophys. J. Lett.*, 886, L27
- Rezaei M., Naderi T., Malekjani M., Mehrabi A., 2020, *Eur. Phys. J. C*, 80, 374
- Riess A. G., 2019, *Nature Rev. Phys.*, 2, 10
- Riess A. G., Casertano S., Yuan W., Macri L. M., Scolnic D., 2019, *Astrophys. J.*, 876, 85
- Riess A. G., Casertano S., Yuan W., Bowers J. B., Macri L., Zinn J. C., Scolnic D., 2020, arXiv:2012.08534
- Sakstein J., Trodden M., 2020, *Phys. Rev. Lett.*, 124, 161301
- Schombert J., McGaugh S., Lelli F., 2020, *Astron. J.*, 160, 71
- Shajib A., et al., 2020, *Mon. Not. Roy. Astron. Soc.*, 494, 6072
- Smith T. L., Poulin V., Amin M. A., 2020, *Phys. Rev. D*, 101, 063523
- Soltis J., Casertano S., Riess A. G., 2020, arXiv:2012.09196
- Vagnozzi S., 2020, *Phys. Rev. D*, 102, 023518
- Valiviita J., Majerotto E., Maartens R., 2008, *JCAP*, 07, 020
- Van De Bruck C., Mifsud J., 2018, *Phys. Rev. D*, 97, 023506
- Verde L., Treu T., Riess A., 2019, *Nature Astron.*, 3, 891
- Wang B., Abdalla E., Atrio-Barandela F., Pavon D., 2016, *Rept. Prog. Phys.*, 79, 096901
- Weinberg S., 2013, *Phys. Rev. Lett.*, 110, 241301
- Wong K. C., et al., 2020, *Mon. Not. Roy. Astron. Soc.*, 498, 1420
- Yang W., Mukherjee A., Di Valentino E., Pan S., 2018a, *Phys. Rev.*, D98, 123527
- Yang W., Pan S., Di Valentino E., Nunes R. C., Vagnozzi S., Mota D. F., 2018b, *JCAP*, 1809, 019
- Yang W., Pan S., Di Valentino E., Saridakis E. N., 2019a, *Universe*, 5, 219
- Yang W., Pan S., Xu L., Mota D. F., 2019b, *Mon. Not. Roy. Astron. Soc.*, 482, 1858
- Yang W., Pan S., Di Valentino E., Saridakis E. N., Chakraborty S., 2019c, *Phys. Rev.*, D99, 043543
- Yang W., Mena O., Pan S., Di Valentino E., 2019d, *Phys. Rev.*, D100, 083509
- Yang W., Pan S., Nunes R. C., Mota D. F., 2020a, *JCAP*, 04, 008
- Yang W., Di Valentino E., Mena O., Pan S., Nunes R. C., 2020b, *Phys. Rev. D*, 101, 083509
- Yang W., Di Valentino E., Mena O., Pan S., 2020c, *Phys. Rev. D*, 102, 023535
- Ye G., Piao Y.-S., 2020, *Phys. Rev. D*, 101, 083507
- Yuan W., Riess A. G., Macri L. M., Casertano S., Scolnic D., 2019, *Astrophys. J.*, 886, 61
- Zeng Z., Yeung S., Chu M.-C., 2019, *JCAP*, 03, 015
- de Jaeger T., Stahl B., Zheng W., Filippenko A., Riess A., Galbany L., 2020, *Mon. Not. Roy. Astron. Soc.*, 496, 3402
- del Campo S., Herrera R., Pavon D., 2009, *JCAP*, 01, 020

This paper has been typeset from a $\text{\TeX}/\text{\LaTeX}$ file prepared by the author.